

## Biocompatibility Assessment of $\text{TiO}_2\text{-CaO-ZrO}_2\text{/HDPE}$ Hybrid Bio-Nanocomposites Used in Bone-Tissue Engineering Scaffolds

Noor A. Al-Mohammedawia\*, Jenan S. Kashan<sup>b</sup>, Shihab A. Zaidan<sup>c</sup>

<sup>a</sup>Department of Biomedical Engineering, University of Technology-Iraq, Baghdad, 10069, Iraq

<sup>b</sup>Department of Biomedical Engineering, University of Technology-Iraq, Baghdad, 10069, Iraq

<sup>c</sup>Department of Applied Sciences, University of Technology-Iraq, Baghdad, 10069, Iraq

\*Corresponding author. Tel.: +964-790-487-4035; E-mail: noor.a.naat@uotechnology.edu.iq

### ABSTRACT

Orthopedic accidents and associated pathologies are a critical global public health issue, as well as a first-rate international burden of incapacity and suffering individuals. Certain injuries and fractures in bone tissue can be complex and lead to residual deformation, necessitating bone replacement. We made new bio-nano composite bone scaffolds in this study by adding nanosized fillers—eight mol%  $\text{CaO-ZrO}_2$  (partially stabilized zirconia) and  $\text{TiO}_2$  (titanium dioxide) to an HDPE (high-density polyethylene) polymeric matrix. We employed the hot-pressing technique to shape the specimens at a compression stress of 29 MPa, a compounding temperature of 150 °C, and a compounding time of 15 minutes. The primary goal is to identify appropriate biocompatibility properties for the nanocomposite  $\text{TiO}_2\text{-CaO-ZrO}_2\text{/HDPE}$ , which could potentially serve as bone replacement materials in bone tissue engineering. We utilized the bioactivity tests to explore and identify biocomposites. To assess the bioactivity and bioavailability of clearly going-on hydroxyapatite, we immersed the specimens in simulated body fluid SBF for various intervals (1, 5, 10) days. Discipline emission scanning electron microscopy (FESEM) and X-ray diffraction (XRD) analyses revealed that every specimen exhibited extremely good bioactivity and formed appetite layers on the sample's surface after immersion in SBF, supporting particle site osteointegration.

**Keywords:** *Biocompatibility, Simulated body fluid (SBF), X-ray diffraction (XRD), Field emission scanning electron microscopy (FESEM), High-density polyethylene (HDPE), Titanium dioxide ( $\text{TiO}_2$ ), Partially stabilized zirconia ( $\text{CaO-PSZ}$ ), Hydroxyapatite (HA)*

### 1. INTRODUCTION

Orthopedic trauma regularly necessitates surgical methods and using biodegradable medical gadgets, along with natural or artificial biomaterials, to replace or repair tissues like ligaments, tendons, cartilage, and bone. The design, usefulness, and bioresponse of those gadgets determine the clinical success of the intervention. Biomaterials are also screened for their innocuity, biocompatibility, protection, and efficacy in scientific settings [1]. Biocompatibility is a vital requirement for the scientific use of biomaterials in orthopedics, inspired by factors that include chemical, mechanical, structural, and interplay with the biological surroundings. The organic evaluation of biomaterials consists of checks related to cytocompatibility, genotoxicity, sensitization, contamination, acute and continual toxicity, hemocompatibility, reproductive and developmental toxicity, carcinogenicity, implantation, and degradation, as specified in international standards. Biocompatibility checking is a primary requirement for the development and approval of orthopedic substances for medical use with the aid of regulatory groups [2].

Animal experiments have tested numerous substances for bone-bonding, implanting them into bone defects and analyzing their bonding to the surrounding bone. Many animals were sacrificed for the duration of those investigations, but there have been no guiding standards for finding bone-bonding substances, especially due to a lack of

awareness of the manner [3]. In 1991, a study cautioned that the capability of a fabric to form apatite in a body fluid that does not cover cells will be used to check its bone-bonding capacity in a lab setting instead of on animals. [4] SBF is widely used for in vitro assessment of bone-bonding functionality in materials. In 2006, researchers summarized correlations between SBF and in vivo animal experiments for numerous substances. [5] In 2007, SBF became standardized as an answer for in vitro assessment of the apatite-forming potential of implant materials under ISO 23317.4. [6] Biomaterials' biocompatibility and tissue responses in difficult tissue may be evaluated through in vitro simulation strategies, animal experiments, and mobile assays. Kokubo's research demonstrates that a biomaterial desires to bind to a residing bone by way of forming bone-like apatite on its surface. In vivo apatite formation may be reproduced by means of immersing the material in a simulated frame fluid (SBF) with similar ion concentrations to human blood plasma. [4]

Kokubo and his colleagues have carried out several research studies on the effectiveness of SBF immersion experiments, focusing on the in vitro apatite-forming capacity of SBF, which considerably impacts osteoconductive. [5,7,8] Biocompatibility has been the subject of several in vitro studies. [9-12] Due to their precise homes, ceramics and polymers have served as difficult-to-tissue alternative materials for many years. Combining these materials can create composites used in numerous

medical applications. The ability to shape them into desired patterns makes polymers the most common. [13] High-density polyethylene (HDPE) is a widely used polyolefin due to its cost-effectiveness, strength, and simplicity of manufacturing, making it perfect for biomedicine due to its bioinert properties. [14] Polyethylene implants' lifespan is confined because of put-on troubles and osteolysis caused by the discharge of PE into the periprosthetic surroundings. [15, 16]. Numerous studies have examined the use of HDPE as a bone alternative in biological applications like orthopedic prostheses and substitutes [17–21]. The study [22] examined the histological and histomorphological responses of porous HDPE tissues. It was observed that the tissues did not exhibit any initial inflammatory reaction and were appropriate for engaging in bone mineral density. The holes were good enough in length and well linked, allowing for a new tissue boom. Various fillers can tailor the physical properties of ceramics and polymer-matrix composites (PMC). [23] TiO<sub>2</sub> nanoparticles are inert, non-poisonous, and cheaper. [24] They are known for their antibacterial and bone-repairing properties, high fracture resistance, ductility, and weight-to-energy ratio. [25], corrosion resistance [26], and chemical balance make them widely used in orthopedics and dentistry. [27]

The literature has explored numerous varieties of polymer-based TiO<sub>2</sub>-composites, which include polyamide/nano-TiO<sub>2</sub> and excessive-effect polystyrene/nano-TiO<sub>2</sub> composites. Zirconia can be stabilized with the aid of oxides like yttrium oxide (Y<sub>2</sub>O<sub>3</sub>), calcium oxide (CaO), or magnesium oxide (MgO) in the course of sintering, resulting in a tetragonal structure at ambient temperature. [28,29] Partially stabilized zirconia (PSZ) is a mixture of zirconia polymorphs created by using inadequate cubic segment-forming oxide (Stabilized), resulting in a cubic and metastable tetragonal ZrO<sub>2</sub> aggregate [29, 30]. Zirconia, a bioceramic substance, is used for bone restoration due to its nontoxicity and biocompatibility. [31] It is likewise used as synthetic bone fillers, orthopedic implants [17, 32], thin films, porous bone scaffolds, and bone cements [37]. They are known for their superior chemical and electrical resistance, refractory characteristics, thermal stability, corrosion and put-on resistance, low friction, excessive mechanical strength, and high thermal growth coefficients. [32-34]

The study critiques the SBF immersion check, a method that evaluates the biocompatibility and tissue responses of biomaterials for tough tissue with the aim of reducing animal use and reducing the duration of the test. It investigates the deposition of apatite calcium phosphates in the TiO<sub>2</sub>-CaO-ZrO<sub>2</sub>/HDPE composite and their mechanism for constructing bone tissue as a hybrid.

## 2. MATERIALS AND METHODS

### 2.1. Materials

#### 2.1.1 High-Density Polyethylene (HDPE)

HDPE powder with particle size of 5 µm and an actual density of (0.941-0.959 g/cm<sup>3</sup>) provided by Right Fortune Industrial Limited (Shanghai, China), was used as a matrix for the composite material.

#### 2.1.2 Titanium Dioxide (TiO<sub>2</sub>)

TiO<sub>2</sub> powder with average particle size of 50 nm and an actual density of (3.9 g/ml) provided by M K Impex Corp. (Canada) was used in this study.

#### 2.1.3 Zirconium Oxide (ZrO<sub>2</sub>) Stabilized with 8mol% Calcia

(PSZ) 8CaO powder with average particle size of 40 nm and real density of (6.0-6.1 g/cm<sup>3</sup>) provided by M K Impex Corp. (Canada) was used in this study.

### 2.2. Materials Characterization Techniques

#### 2.2.1. X-ray Diffraction (XRD)

X-ray diffraction is a non-destructive analytical technique used to identify inorganic and organic crystalline materials. The biocomposite specimens (TiO<sub>2</sub>-CaO-ZrO<sub>2</sub>/HDPE) were analyzed using SHIMADZU XRD 6000 under specific conditions such as a voltage of 40 kV, current of 30 mA, drive axis of -2, scan speed of 10.0000 °/min, sampling pitch of 0.2000 °, and preset time of 1.20 s.

#### 2.2.2. Morphological Examination (Field Emission Scanning Electron Microscopy (FESEM))

The morphology of composite material specimens was examined using Field Emission Scanning Electron Microscopy (FESEM) at an accelerated voltage of 3–10 kV at the College of Science/University of Basra/Iraq. To prevent heat build-up and electrostatic charging, the specimens were coated with a thin layer of gold under vacuum before the FESEM investigation.

### 2.3. Production of the Hybrid Bio Composite Specimens

Hybrid bio-nano composites were prepared as shown in Figure 1. Weighed the composite powders using precision balances and mixed them using roll ball milling with three ceramic balls, each with a diameter variation of 2.2 cm, to ensure a uniform particle distribution in the composites. Set the roll ball milling's rotational velocity to 11.09 Hz, which is approximately 665 rpm. The mixing time extended to 2 hrs, during which all specimens were ready for use. We then used the hot-pressing technique to create the composite specimens. Apply 29 MPa, a temperature of 150 °C, and a speed of 0.5 mm/min to the powder mold for 15 minutes to form the specimens. We gradually release the pressure until the specimens cool down, resulting in a disk-shaped disk

with a diameter of 14.7 mm and a height of seven to 10 mm. Therefore, the total number of specimens was 9, as demonstrated in Table 1. Each specimen is fabricated under

the same conditions: temperature degree, heating duration, and compression speed.

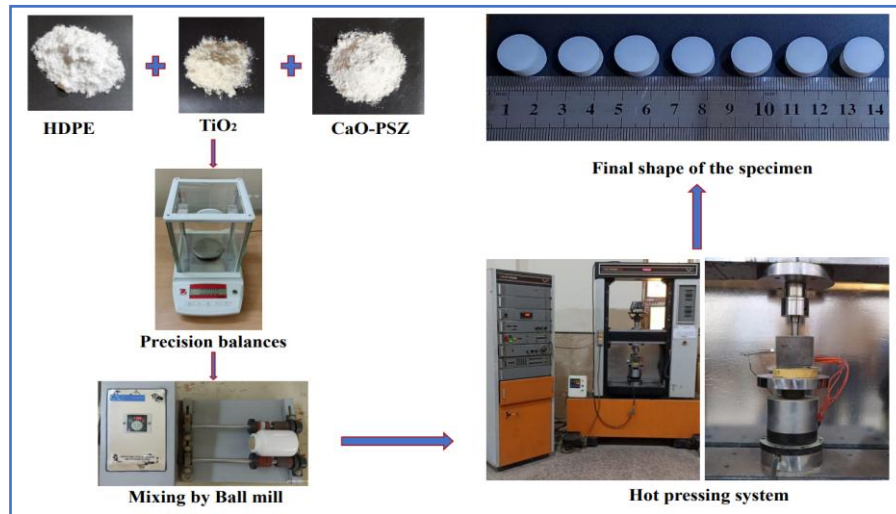


**Figure 1.** Production of hybrid bio-nano composites.

**Table 1** The selected composition of specimens prepared in this study

HDPE (wt. %)	TiO <sub>2</sub> (wt. %)	CaO-PSZ (wt. %)
90	5	5
85	5	10
80	5	15
85	10	5
80	10	10
75	10	15
80	15	5
75	15	10
70	15	15

## 2.4. Preparation of Simulated Body Fluids (SBF)

Kokubo and his crew created an acellular simulated body fluid (SBF) with the same amount of inorganic ions as human extracellular fluid so that they could make apatite on bioactive materials in vitro. This fluid, using the biocompatibility test system shown in Figure 2, can check the bioactivity of man-made materials and cover different substances with apatite in biomimetic conditions. Table 2 presents the ion concentrations of SBF.

To clean the bottles, use a pipette to add 10 ml of hydrochloric acid solution at a concentration of 0.1 mol, then place it in a glass box with 1 L of distilled water to dilute the solution to a concentration of 0.001 M. Immerse the bottles in a dilute hydrochloric acid solution for 2–3 hours, then wash them with deionized water more than

once and cover their mouths with a film. If wished, dry them in a dryer at 50 °C, place 750 mL of deionized water in a 1,000 mL beaker, and stir it at 36 °C with a magnetic stirrer and heater. To avoid dirt, place the beaker on a clean bench. Once each chemical in Table 2 has completely dissolved in the water, add 250 mL of deionized water to 750 mL, resulting in a volume of 1000 mL. Add 1 kmol/dm<sup>3</sup>-HCl solution gradually, ensuring less than 1 g to avoid a local pH increase. To regulate the pH of a solution, calibrate a pH meter with a sparkling popular buffer solution and measure its pH at 36.5 °C. Titrate the 1 kmol/dm<sup>3</sup>-HCl solution with a pipette to adjust the pH to 7.25 or 7.40. Transfer the solution to a tumbler volumetric flask, wash the interior with deionized water, and add the solution. Adjust the amount to a thousand mL, shake well, and preserve it in bottles at room temperature till the solution reaches 20 °C. After cooling.

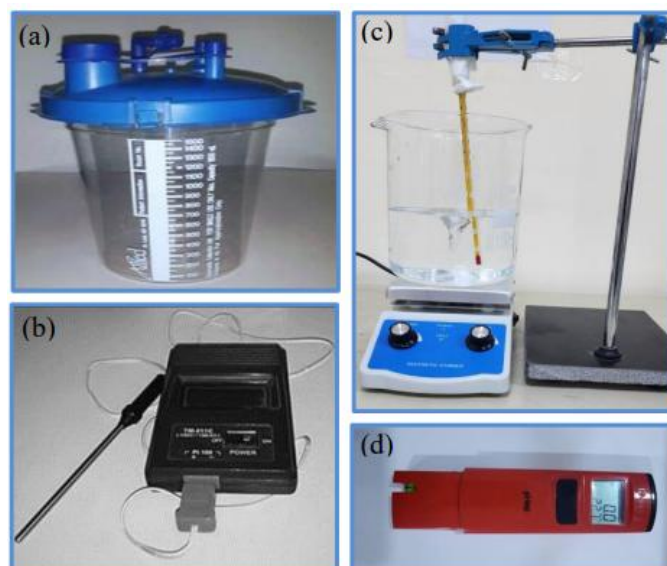


**Figure 2.** Biocompatibility test system a) Pyrex container with cover b) Thermometer c) Simulated body fluid solution with a magnetic stirrer and heater d) PH-meter type HANNA.

**Table 2** Amounts of Reagents for Preparation of SBF [35]

Item	Reagents	Simulated Body Fluid (SBF) 1000mL	Human Blood Plasma 1000mL
1	Sodium chloride (NaCl)	7.996 g	11.994g
2	Sodium bicarbonate (NaHCO <sub>3</sub> )	0.350g	0.525g
3	Potassium chloride (KCl)	0.224g	0.336g
4	Potassium phosphate dibasic trihydrate (K <sub>2</sub> HPO <sub>4</sub> )	0.228g	0.342g
5	Magnesium chloride hexahydrate (MgCl <sub>6</sub> .H <sub>2</sub> O)	0.305g	0.458g
6	Calcium chloride (CaCl <sub>2</sub> .H <sub>2</sub> O)	0.278g	0.417g
7	Sodium sulfate (Na <sub>2</sub> SO <sub>4</sub> )	0.071g	0.107g
8	1 kmol/dm <sup>3</sup> HCl	Appropriate amount for adjusting pH	

## 2.5. Biocompatibility Test (In-Vitro Test)

When selecting and utilizing orthopedic implants, there are important factors to consider. In terms of bioactivity, natural bone nucleation and growth on the orthopedic implant are key parameters that accelerate damage treatment and reduce healing time. [7] In vitro, a material's bioactivity can be tested by immersing it in simulated frame fluid (SBF), which contains ions similar to those in human blood plasma. This is a common way to test the bioactivity of synthetic materials. [36,4]. Table 2 lists the components of the SBF solution. The study's goal was to find out how bioactive the samples were by putting them in 500 mL of SBF that had its pH raised to 7.4 with HCl. Three immersion times were considered (1, 5, and 10 days), and the specimens were left in a laboratory incubator at 37°C. After each incubation, we dried the specimens and used XRD and FESEM tests to determine the amount of hydroxyapatite (HA) formed and its bioactivity.

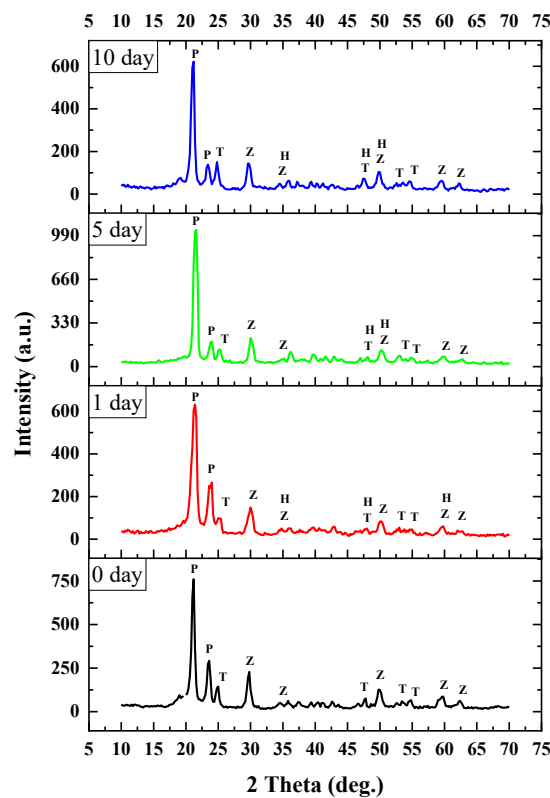
## 3. RESULTS AND DISCUSSION

### 3.1. XRD Analysis

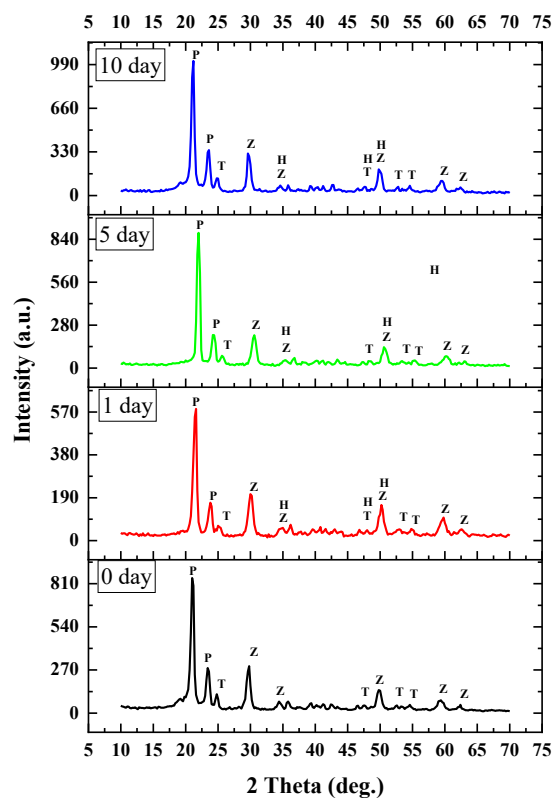
The XRD technique is an additional analysis of bioactivity aspects. The study's goals were to find out what kinds of phases and structures are in HA and to look at the bioactivity of a composite (TiO<sub>2</sub>-CaO-ZrO<sub>2</sub>/HDPE) before and after it was put into a solution that was like natural blood plasma. Different immersion times (1, 5, and 10 days) are shown in Figure 10. The characteristic peaks of HDPE show (2θ) (21.2°, 23.6°, 39.6°, 40.4°, 41.2°) corresponding to the reflection planes (hkl) (110), (200), (011), (310), (111), respectively. They are linked to the JCPDS (Joint Committee on Powder Diffraction Standards) card with the file number 53-1859. The XRD peaks of HDPE were looked at in different places. The unique peaks in TiO<sub>2</sub> were found in (2θ) (25.2°, 36.2°, 37.4°, 47.8°, 52.8°, 54.6°) and were matched to the reflection planes (hkl) (101), (103), (004), (200), (105), and (211), according to the standard XRD form JCPDS card file number (21-1272). As for the characteristic peaks of ZrO<sub>2</sub>, show (2θ) (29.2°, 30°, 34.8°, 42.8°, 43.8°, 46.6°, 50.2°, 57.2°, 59.8°, 62.6°) corresponding to the

reflections planes (hkl) (101), (111), (200), (102), (112), (202), (220), (113), (311), (222), respectively. The occurrence of the cubic phase in reflection planes (hkl) (111), (200), (220), (311), (222), the tetragonal phase in (101), (102), (112), and the monoclinic phase in (202), (113) serve as markers for the significant peaks of the  $\text{ZrO}_2$  phase. The significant peaks that appeared according to the standard XRD form JCPDS card file numbers were (27-0997), (37-1484), and (42-1164). It can be observed that the effect of SBF on the immersion time caused a slight shift in  $2\theta$ . This proves the stability of the components of the composites during their exposure to SBF. In the XRD analysis, prominent peaks at  $2\theta$  values were observed, confirming the presence of HA. A slight increase in main

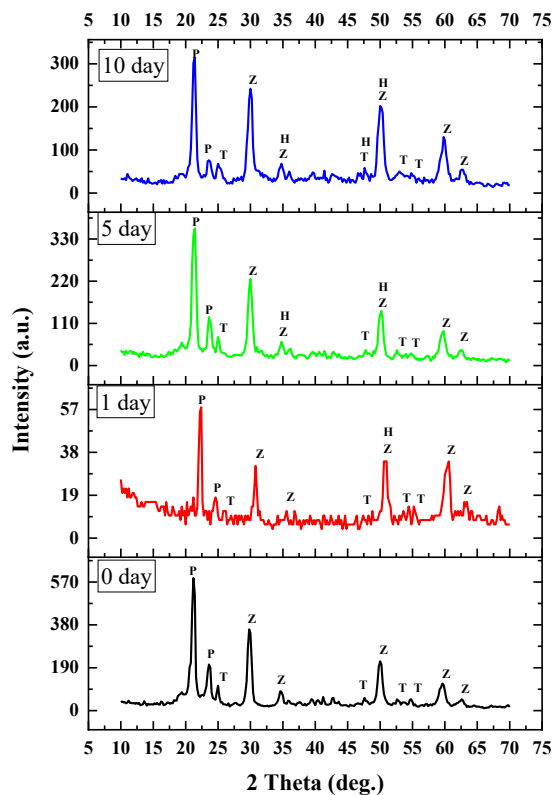
peaks at  $2\theta$  values of  $34.8^\circ$ ,  $47.8^\circ$ , and  $50.2^\circ$  corresponding to the reflections planes (hkl) (202), (222), and (213) respectively, qualitative evaluation of the diffraction patterns adapted by JCPDS reference standard JCPDS-01-074-9762 [37]. After 1, 5, and 10 days of immersion, it indicated the formation of a layer of HA from the SBF on the surface. The study found that exposing a specimen to an SBF solution increased the HA value, forming precipitates that aid in implant attachment to bone. Zirconia nanoparticles made the composite system more stable, giving hydroxyapatite more time to form bioactive bonds with bone cells. Improved stability of the composite system enhanced hydroxyapatite's ability to form bioactive bonds with bone cells.[9]



(a) 90%HDPE - 5%TiO<sub>2</sub> - 5% CaO-ZrO<sub>2</sub>

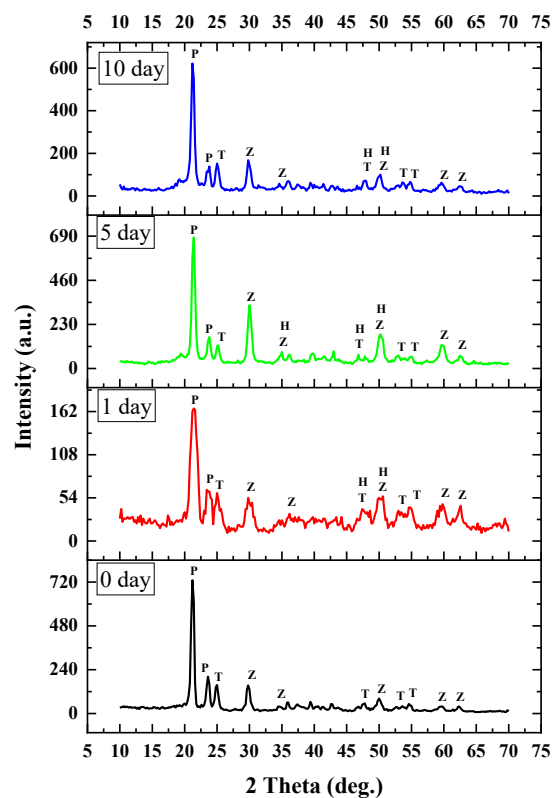


(b) 85%HDPE - 5%TiO<sub>2</sub> - 10% CaO-ZrO<sub>2</sub>

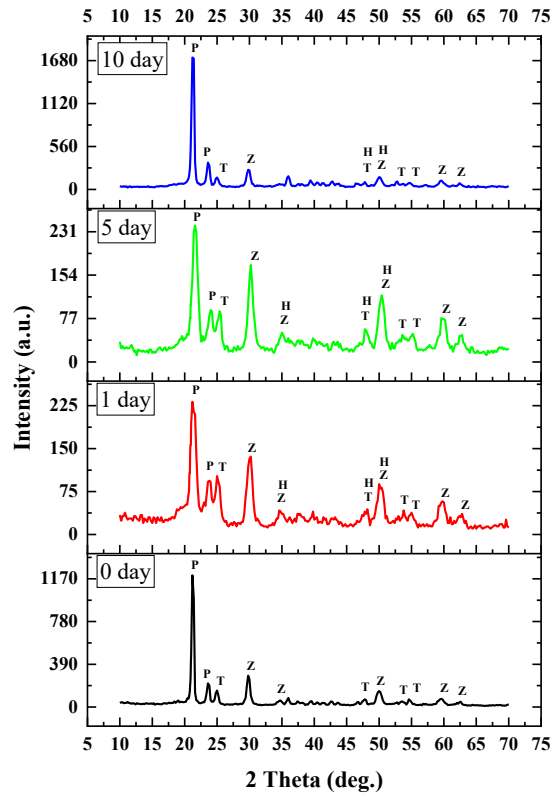


(c) 80%HDPE - 5%TiO<sub>2</sub> - 15% CaO-ZrO<sub>2</sub>

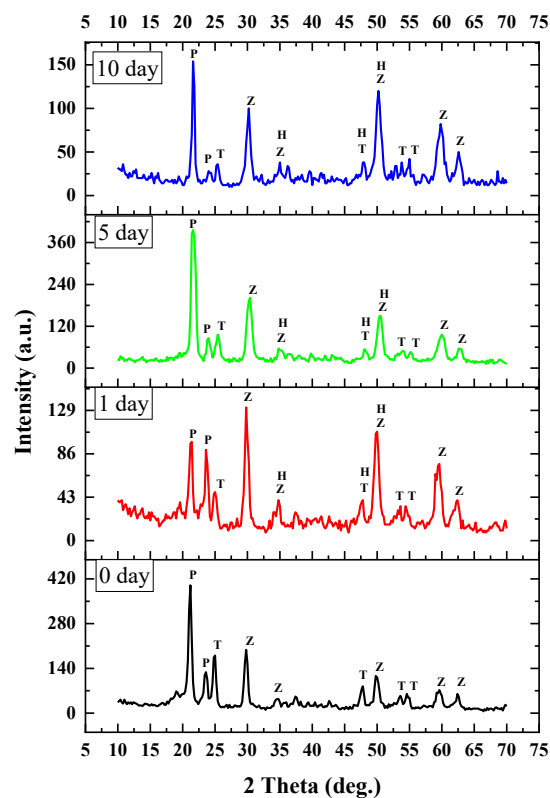




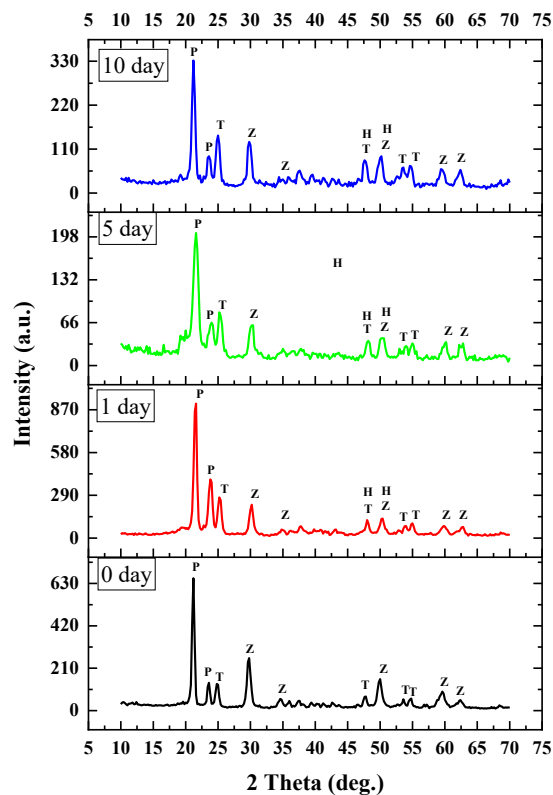
d) 85%HDPE -10%TiO<sub>2</sub> - 5% CaO-ZrO<sub>2</sub>



(e) 80%HDPE -10%TiO<sub>2</sub> -10% CaO-ZrO<sub>2</sub>

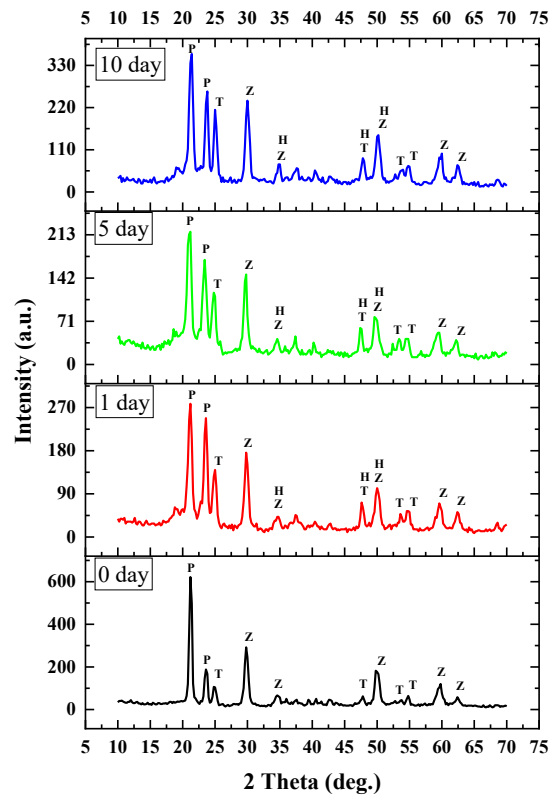


(f) 75%HDPE -10%TiO<sub>2</sub> -15% CaO-ZrO<sub>2</sub>

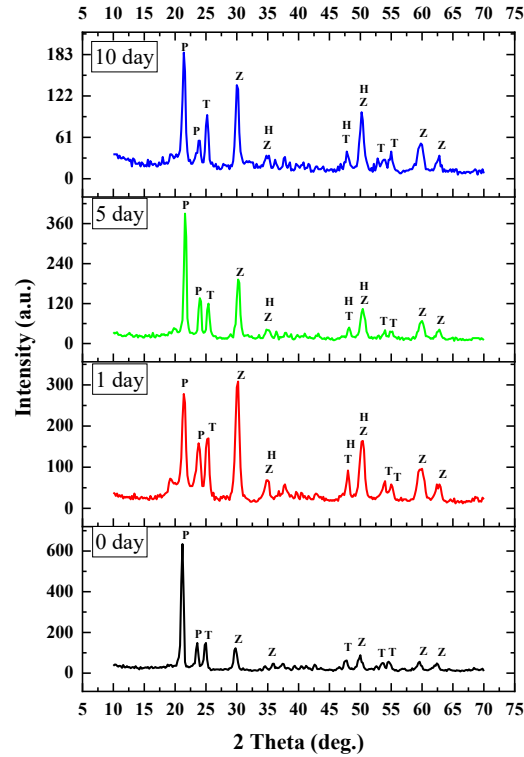


(g) 80%HDPE -15%TiO<sub>2</sub> - 5% CaO-ZrO<sub>2</sub>





(h) 75%HDPE -15%TiO<sub>2</sub> -10% CaO-ZrO<sub>2</sub>



(i) 70%HDPE -15%TiO<sub>2</sub> - 15%CaO-ZrO<sub>2</sub>

**Figure 3.** XRD plots for (TiO<sub>2</sub>-CaO-ZrO<sub>2</sub>/HDPE) composite materials specimen's composite: a) before immersion, b) after 1 day, c) after 5 days and d) after 10 days of immersion in SBF's solution the abbreviations (P, T, Z, H) denote (HDPE, TiO<sub>2</sub>, CaO-ZrO<sub>2</sub>, HA), respectively.

### 3.2. FESEM Analysis

To recognize apatite formation on the composite's surface, we performed FE-SEM analysis before the immersion day and after 1, 5, and 10 days of immersion in SBF's solution. The FE-SEM pictures of the biocomposite surfaces (TiO<sub>2</sub>-CaO-ZrO<sub>2</sub>/HDPE) revealed that all specimens had a smooth, even surface prior to their immersion in SBF. The specimens deposited the HA layer on their surfaces after immersion in SBF; they developed a new "cauliflowerlike" structure of apatite crystals, indicating the formation of the appetite layers on the sample's surface. Also, we can see that the amount of HA layer developed with the increasing immersion time from 1–10 days; this is in agreement with a

previous investigation. [38] The FE-SEM analysis reveals that increasing the growth of HA films on the composite surfaces creates the best bioactivity. [39] This helps with osseointegration and avoids fibrous encapsulation. [40] To better understand a specimen's surface bioactivity, The bioactivity test result was in agreement with the findings from the FE-SEM. It was shown that all of the TiO<sub>2</sub>-CaO-ZrO<sub>2</sub>/HDPE composites were bioactive because they could cause hydroxyapatite to form from the SBF. The HA layer covered the composite surface, proving the specimen's excellent bioactivity characteristics as a substitute material for bone repair, which was in agreement with the conclusions reported by other studies. [36,11]

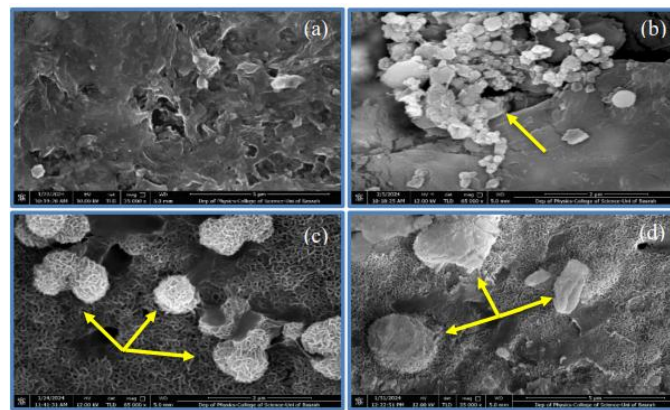


**Figure 4.** FE-SEM images of the (90%HDPE - 5%TiO<sub>2</sub> - 5% CaO-ZrO<sub>2</sub>) Composite: a) before immersion, b) after 1 day, c) after 5 days and d) after 10 days of immersion in SBF's solution (the yellow arrows indicate the HA layers).

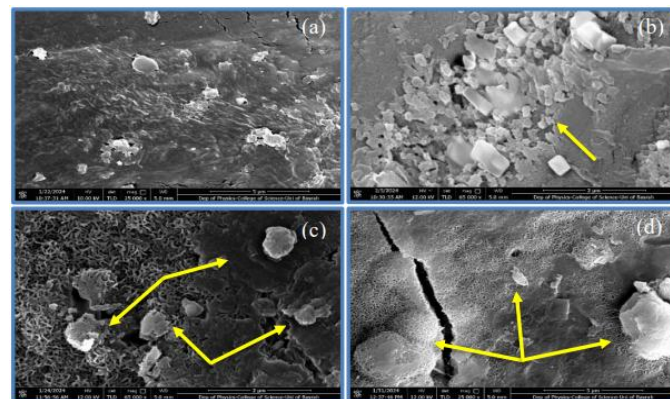


**Figure 5.** FE-SEM images of the (85%HDPE - 5%TiO<sub>2</sub> - 10%CaO-ZrO<sub>2</sub>) Composite: a) before immersion, b) after 1 day, c) after 5 days and d) after 10 days of immersion in SBF's solution (the yellow arrows indicate the HA layers).

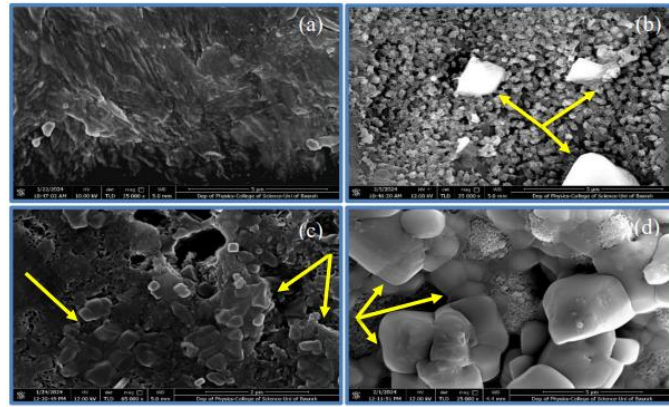


**Figure 6.** FE-SEM images of the (80%HDPE- 5%TiO<sub>2</sub>- 15% CaO-ZrO<sub>2</sub>) Composite: a) before immersion, b) after 1 day, c) after 5 days and d) after 10 days of immersion in SBF's solution (the yellow arrows indicate the HA layers).

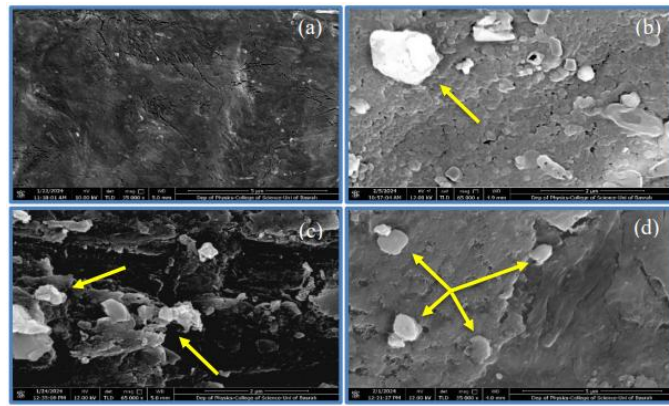


**Figure 7.** FE-SEM images of the (85%HDPE -10%TiO<sub>2</sub> - 5%CaO-ZrO<sub>2</sub>) Composite: a) before immersion, b) after 1 day, c) after 5 days and d) after 10 days of immersion in SBF's solution (the yellow arrows indicate the HA layers).

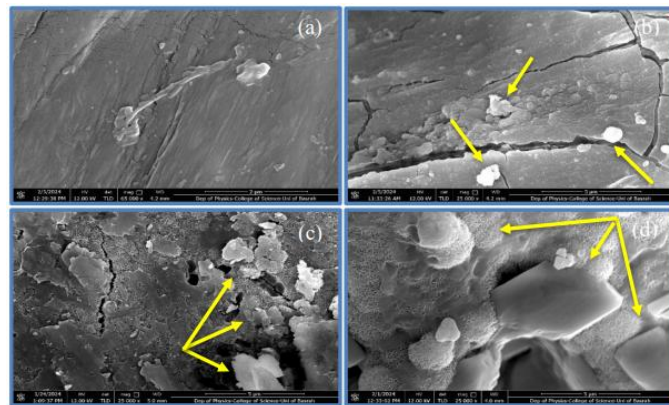


**Figure 8.** FE-SEM images of the (80%HDPE -10%TiO<sub>2</sub> -10%CaO-ZrO<sub>2</sub>) Composite: a) before immersion, b) after 1 day, c) after 5 days and d) after 10 days of immersion in SBF's solution (the yellow arrows indicate the HA layers).

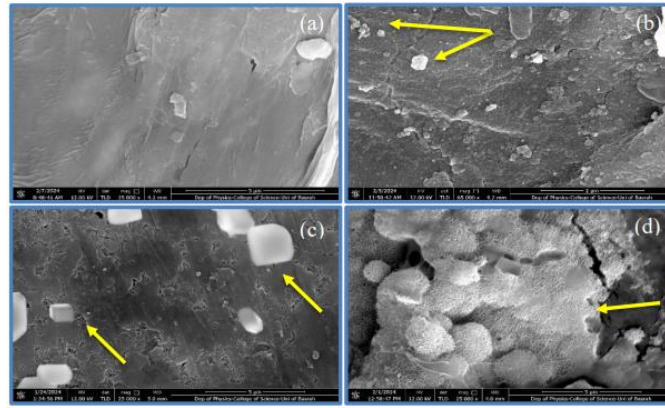


**Figure 9.** FE-SEM images of the (75%HDPE -10%TiO<sub>2</sub> -15%CaO-ZrO<sub>2</sub>) Composite: a) before immersion, b) after 1 day, c) after 5 days and d) after 10 days of immersion in SBF's solution (the yellow arrows indicate the HA layers).

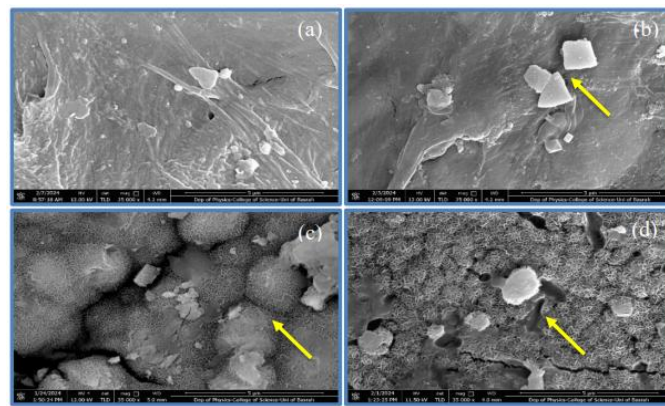


**Figure 10.** FE-SEM images of the (80%HDPE -15%TiO<sub>2</sub> - 5%CaO-ZrO<sub>2</sub>) Composite: a) before immersion, b) after 1 day, c) after 5 days and d) after 10 days of immersion in SBF's solution (the yellow arrows indicate the HA layers).

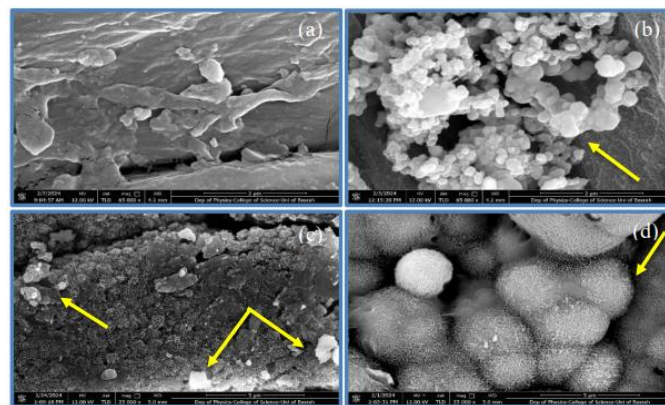


**Figure 11.** FE-SEM images of the (75%HDPE -15%TiO<sub>2</sub> -10%CaO-ZrO<sub>2</sub>) Composite: a) before immersion, b) after 1 day, c) after 5 days and d) after 10 days of immersion in SBF's solution (the yellow arrows indicate the HA layers).



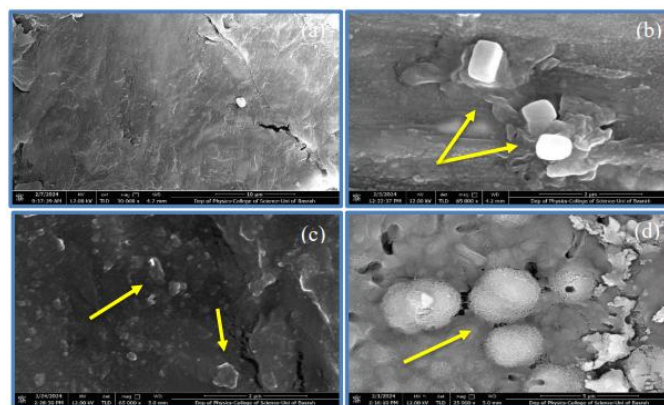


**Figure 12.** FE-SEM images of the (70%HDPE - 15%TiO<sub>2</sub> - 15%CaO-ZrO<sub>2</sub>) Composite: a) before immersion, b) after 1 day, c) after 5 days and d) after 10 days of immersion in SBF's solution (the yellow arrows indicate the HA layers).

#### 4. CONCLUSION

The bioactivity tests exhibited the formation of appetite layers on the specimen's surface after one day of immersion in SBF. This layer also developed with an increase in immersion time after 5 and 10 days of immersion, as confirmed by XRD and FESEM. Based on the XRD data, prominent peaks at  $2\theta$  values were observed, confirming the presence of HA after immersion in SBF and the formation of appetite layers on the specimen's surface. It can be observed that the effect of SBF on the immersion time caused a slight shift in  $2\theta$ . This proves the stability of the components during their exposure to SBF. The FE-SEM analysis reinforces this result, revealing that increasing the growth of HA films on the composite surfaces after immersion in SBF leads to the creation of the best bioactivity. All specimens demonstrate good bioactivity, indicating that the TiO<sub>2</sub>-CaO-ZrO<sub>2</sub>/HDPE biocomposite holds great potential for use as a bone substitute material.

#### ACKNOWLEDGMENTS

Praise be to Allah for everything. I am grateful to everyone who has given me the support I needed to complete this work.

#### REFERENCES

- [1] Assad M and Jackson N: Biocompatibility evaluation of ortho- pedic biomaterials and medical devices: A review of safety and efficacy models. In: Encyclopedia of Biomedical Engineering. Vol 2. 1st edition. Narayan RJ (ed). Elsevier, Amsterdam, pp281-309, 2019.
- [2] Helmus MN, Gibbons DF and Cebon D: Biocompatibility: Meeting a key functional requirement of next-generation medical devices. Toxicol Pathol 36: 70-80, 2008.
- [3] Tadashi Kokubo, Seiji Yamaguchi, "Simulated body fluid and the novel bioactive materials derived from it", JOURNAL OF BIOMEDICAL MATERIALS RESEARCH PART A", 2019.
- [4] Kokubo, Tadashi. "Bioactive glass ceramics: properties and applications." Biomaterials 12, no. 2 (1991): 155-163.
- [5] T. Kokubo and H. Takadama, "How useful is SBF in predicting in vivo bone bioactivity?" Biomaterials, vol. 27, no. 15, pp. 2907– 2915, 2006.
- [6] Implants for Surgery-In Vitro Evaluation for Apatite-Forming Ability of Implant Materials. International Standards, ISO/FDIS 23317; 2007.
- [7] S. Fujibayashi, M. Neo, H.-M. Kim, T. Kokubo, and T. Nakamura, "A comparative study between in vivo bone ingrowth and in vitro apatite formation on Na<sub>2</sub>O-CaO-SiO<sub>2</sub> glasses," Biomaterials, vol. 24, no. 8, pp. 1349–1356, 2003.
- [8] S. Yamaguchi, H. Takadama, T. Matsushita, T. Nakamura, and T. Kokubo, "Preparation of bioactive Ti-15Zr-4Nb-4Ta alloy from HCl and heat treatments after an NaOH treatment," Journal of Biomedical Materials Research Part A, vol. 97, no. 2, pp. 135–144, 2011.
- [9] J. S. Kashan, "Preparation and Characterization of Hydroxyapatite/ Yttria Partially Stabilized Zirconia Polymeric Biocomposite", PhD thesis, University of Technology, 2014.
- [10] Y. Akgul, H. Ahlatci, M. E. Turan, H. Simsir, M. A. Erden, Y. Sun, A. Kilic, Polym. Compos. 2020, 41, 2426.
- [11] Ali A. Al-allaq, Jenan S. Kashan, Mohamed T. El-Wakad, Ahmed M. Soliman, EVALUATION OF A HYBRID BIOCOMPOSITE OF HA/HDPE REINFORCED WITH MULTI-WALLED CARBON NANOTUBES (MWCNTs) AS A BONE-SUBSTITUTE MATERIAL", Materiali in tehnologije / Materials and technology 55 (2021) 5, 673–680.
- [12] M. L. Wang, N. Y. Xu, R. Z. Tang, X. Q. Liu, Mater Today Bio. 2022, 15, 1.
- [13] Dhabale, R., & Jatti, V. S. (2016, September). A bio-material: mechanical behaviour of LDPE-Al<sub>2</sub>O<sub>3</sub>-TiO<sub>2</sub>. In IOP Conference Series: Materials Science and Engineering (Vol. 149, No. 1, p. 012043). IOP Publishing.
- [14] Hermán, V., Karam, A., Albano, C., & González, G. (2015). High density polyethylene-hydroxyapatite composites synthesized by in situ ethylene polymerization. Revista de la Facultad de Ingeniería Universidad Central de Venezuela, 30(1), 211-218.
- [15]

- [16] Jakub Z, Matsu R, Martin V, Jiří G, Ivan K, and Martin H, 2018 UHMWPE acetabular cup creep deformation during the run-in phase of THA's life cycle, *Journal of the Mechanical Behavior of Biomedical Materials*, 87, 30-39.
- [17] Shahemi N, Liza S, Abbas A. and Merican A M., 2018 Long-term wear failure analysis of UHMWPE acetabular cup in total hip replacement, *Journal of the Mechanical Behavior of Biomedical Materials*, 87, 1-9.
- [18] Noor A. Al-Mohammedawi, Shihab A. Zaidan, Jenan S. Kashan, "Preparation and Characterization of TiO<sub>2</sub>-CaO-ZrO<sub>2</sub>/HDPE Hybrid Bio-Nanocomposites for Use in Orthopedic Applications", *International Information and Engineering Technology Association*, Vol. 48, No. 1, February, pp. 43-55, 2024.
- [19] AL-ALLAQ, A. L. I. A., Jenan S. Kashan, Mohamed T. El-Wakad, and Ahmed M. Soliman. "HA/HDPE Reinforced with MWCNTs for Bone Reconstruction and Replacement Application." *Materiale Plastice* 59, no. 1 (2022).
- [20] Kashan, Jenan S. "Optimization Using Taguchi Method for Physical and Mechanical Properties of Bio Mimicking Polymeric Matrix Composite for Orthodontic Application." *Engineering and Technology Journal* 37, no. 5A (2019): 181-187.
- [21] Xu, J.; Hu, X.; Jiang, S.; Wang, Y.; Parungao, R.; Zheng, S.; Nie, Y.; Liu, T.; Song, K. The Application of Multi-Walled Carbon Nanotubes in Bone Tissue Repair Hybrid Scaffolds and the Effect on Cell Growth in Vitro. *Polymers*. 2019, 11, 230.
- [22] Balakrishnan, H.; Husin, M. R.; Wahit, M. U.; Abdul Kadir, M. R. Preparation and Characterization of Organically Modified Montmorillonite-Filled High Density Polyethylene/Hydroxyapatite Nanocomposites for Biomedical Applications. *Poly.-Plast. Technol. Eng.* 2014, 53, 790–800.
- [23] Martínez Rodríguez, J.; Renou, S. J.; Guglielmotti, M. B.; Olmedo, D. G. Tissue Response to Porous High Density Polyethylene as a Three-Dimensional Scaffold for Bone Tissue Engineering: An Experimental Study. *J. Biomater. Sci. Polym. Ed.* 2019, 30, 486– 499.
- [24] Thomas H. and Dorothée, V. S., *Polymer-Nanoparticle Composites: From Synthesis to Modern Applications*, *Materials*, Vol. 3, (2010), pp. 3468-3517.
- [25] Daniela Y, Sichem G, Ingo L, María T U, Tatiana G, Franco M R. and Paula A Z, 2015 Photocatalytic inhibition of bacteria by TiO<sub>2</sub> nanotubes-doped polyethylene composites, *Applied Catalysis A: General*, 489, 255–261.
- [26] Khaled, S. M., Sui, R., Charpentier, P. A., & Rizkalla, A. S., *Langmuir*, 2007, 23(7), 3988–3995.
- [27] Lai, Y., Cheng, Y., Yang, H., Yang, Y., Huang, J., Chen, Z., Wang, X., Lin, C. (2018). Progress in TiO<sub>2</sub> nanotube coatings for biomedical applications: A review. *Journal of Materials Chemistry B*, 6: 1862-1886.
- [28] Imran, M., Riaz, S., & Naseem, S. *Materials Today*, Elsevier Ltd. (2012), *Proceedings* (Vol. 2).
- [29] Thamaraiselvi, T. and Rajeswari, S., 2004. Biological evaluation of bioceramic materials a review. *Carbon*, 24(31), p.172.
- [30] Abed, Hafidh Yousif, Mohammad Almasi-Kashi, and Shihab Ahmed Zaidan. "Structural Properties of Yttria Stabilized Zirconia With Different Nano Alumina-Magnesia Spinel Additions." In *Journal of Physics: Conference Series*, vol. 1178, no. 1, p. 012035. IOP Publishing, 2019.
- [31] Fu, L., Khor, K.A. and Lim, J.P., 2001. Processing, microstructure and mechanical properties of yttria stabilized zirconia reinforced hydroxyapatite coatings. *Materials Science and Engineering: A*, 316(1-2), pp.46-51.
- [32] [31] S. S. Raghavendra, G. R. jadhav, K. M. Gathani, P. Kotadia, "bioceramics in endodontics – a review", *J. Istanbul Univ. Fac. Dent.*, 51, pp. S128-S137, 2017.
- [33] Afzal, Adeel. "Implantable zirconia bioceramics for bone repair and replacement: A chronological review." *Materials Express*, Vol. 4, No. 1, 2014, pp. 1-12.
- [34] José F B Anton S, Heinz-Dieter K, Janet G, and Frank A M, 2016 New ZrO<sub>2</sub>/Al<sub>2</sub>O<sub>3</sub> Nanocomposite Fabricated from Hybrid Nanoparticles Prepared by CO<sub>2</sub> Laser Co-Vaporization, *Nature scientific reports*, 1-11.
- [35] Thirupathy M, Dhanapal B, and Suresh S, 2016 Synthesis and Characterization of Yttrium Stabilized Zirconia Nanoparticles, *Materials Research*, 19, 4, 812-816.
- [36] Satomi Suzuki 'FABRICATION OF HYDROXYAPATITE-BIODEGRADABLE POLYMER SCAFFOLDS BY ELECTROSPINNING FOR POTENTIAL BONE TISSUE APPLICATION"', Submitted to the Faculty of New Jersey Institute of Technology, 2006.
- [37] Kokubo, Tadashi. "Apatite formation on surfaces of ceramics, metals and polymers in body environment." *Acta materialia* 46, no. 7 (1998): 2519-2527.
- [38] A. D. Anastasiou, C. L. Thomson, S. A. Hussain, T. J. Edwards, S. Strafford, M. Malinowski, R. Mathieson, C. T. A. Brown, A. P. Brown, M. S. Duggal, A. Jhaa "Sintering of calcium phosphates with a femtosecond pulsed laser for hard tissue engineering" *Materials & Design* 101, pp.346-354, 2016.
- [39] H. Balakrishnan, M. R. Husin, M. U. Wahit, M. R. Abdul Kadir, Preparation and characterization of organically modified montmorillonite-filled high-density polyethylene/hydroxyapatite nanocomposites for biomedical applications, *Polym. Plast. Technol. Eng.*, 53 (2014) 8, 790–800.
- [40] M. R. Husin, M. U. Wahit, M. R. Abdul Kadir, W. A. Wan Abd. Rahman, Effect of hydroxyapatite reinforced high density polyethylene composites on mechanical and bioactivity properties, *Key Engineering Materials*, 471 (2011), 303–308.
- [41] R. A. Sousa, R. L. Reis, A. M. Cunha, M. J. Bevis, Processing and properties of bone-analogue biodegradable and bioinert polymeric composites, *Compos. Sci. Technol.*, 63 (2003), 3–4, 389–402.